

Topotactic conversion of Ni₃CuN into Ni₃Cu with Anti-Perovskite Structure Reveals the Role of Nitrogen on Electrocatalytic Properties

Zhengxin Yang^a, Angela Daisley^a, Christopher Kelly^a, Justin S. J. Hargreaves^a, Alexey Y. Ganin^a

*

a. School of Chemistry, University of Glasgow, Glasgow, G12 8QQ, United Kingdom

* Corresponding Author

Experimental

1.1 The synthesis of Ni₃CuN and Ni₃Cu

0.352 g (6 mmol) of Ni metal (99.9%, Thermo Fisher Scientific) and 0.187 g (2 mmol) of Cu (99.9%, Thermo Fisher Scientific) powders were mixed in the stoichiometric ratio. The mixture was sandwiched between two silica wool pieces within a quartz tube (8 × 230 mm). The tube was then inserted into a separate quartz tube (acting as a flow bed reactor). This tube was inserted vertically into a tube furnace. Subsequently, the system was heated at 500 °C (5 °C/min) for 6 h and then at 560 °C (5 °C/min) for 6 h under a flow rate of NH₃ of 95 mL/min. After the mixture cooled to room temperature, the material was passivated using a mixture of 2 % O₂/Ar at 25 mL/min and further diluted with N₂ for 1 hour. Finally, the resulting dark grey powder was ground with a pestle and mortar.

Ni₃Cu was prepared from Ni₃CuN as a precursor. 300 mg of Ni₃CuN were sandwiched between two silica wool pieces within a quartz tube (10 × 50 mm). The tube was placed horizontally into a quartz tube within the tube furnace and then heated at 400 °C for 6 h under the flow of 5% H₂/Ar gas mixture (100 ml/min flow rate) with 5 °C/min heating and cooling rates. Finally, the resulting grey powder was ground with a pestle and mortar.

1.2 Characterization

Powder X-ray diffraction (PXRD) was conducted on a Rigaku MiniFlex 6G equipped with a D/teX Ultra detector and Cu-source (K_{α1} and K_{α2} wavelengths are 1.5406 and 1.5444 Å, respectively) operating in the Bragg-Brentano geometry. Before the measurement, samples were immobilised on zero background holders and flattened with glass microscope slides. Diffraction patterns were collected with a step size of 0.015° and a scanning rate of 3°/min. GSAS-II software was also employed to perform the Rietveld refinements of PXRD data, including the unit cell parameter, the sample displacement, the microstrain, and the crystal size. The background was fitted using the shifted Chebyshev polynomial shape.

Microanalysis was used to reveal nitrogen content in the as-prepared Ni₃CuN by an Exeter CE-440 Elemental Analyser. On this analyser, samples are weighed in duplicate, ranging from 1.6 mg to 1.9 mg, into tin capsules and loaded into the sample wheel, along with several calibration standards and elemental blanks. The capsules are then combusted at around 975°C, and the resulting gases travel

through both a combustion and reduction tube, where all metals and oxides are removed. The gas then passes through several mixing stages with pure oxygen to ensure that only CO₂, H₂O, N₂, and helium remain in the system. The gases pass through a CO₂ trap and an H₂O trap, where their respective compounds are removed. Detectors at the end of each trap take a microvolt charge of how much gas is removed, and the system uses the molecular mass of each to determine the Carbon and Hydrogen charges without the Oxygen attached. Finally, the only gases that are left are N₂ and Helium, so an N₂ detector at the end of the system detects the charge, and the instrument divides the value by 2 to get the Nitrogen charge. Once the run is complete, the system uses the following equation to find the wt. % of Carbon, Hydrogen, and Nitrogen in 1 μg of the sample.

Elemental wt. % = Calibration Factor × (Elemental Charge - Blank Capsule Charge) / Mass of Sample

X-ray fluorescence (XRF) was performed on a Rigaku NEX DE series. Powder samples were placed on the holders and made flat using the adjustable die punch before measuring the ratio of the metal elements.

Scanning Electron Microscopy (SEM) and Energy Dispersive X-ray Spectroscopy (EDS) were performed with a TESCAN CLARA instrument equipped with an Oxford Instruments UltimMax 65. The sample (1 mg) was evenly distributed on a 9 mm adhesive carbon tab (Agar Scientific) with a spatula, followed by shaking it to remove the excess powder. Then, the disk was attached to a SEM specimen stub (Agar Scientific) and sputter-coated (Agar Sputter Coater) with gold for 30 s before the measurement.

X-ray Photoelectron Spectroscopy (XPS) was carried out using a Kratos AXIS Supra⁺ spectrometer with a monochromated Al K alpha X-ray source operating at 1486.6 eV. The high-resolution spectra were recorded at the pass energy of 50 eV and energy resolution of 0.1 eV. The analysed area was 0.66 mm². The powders were uniformly dispersed as a thin layer onto an adhesive carbon tab (Agar Scientific) and affixed to the sample holder before the measurements.

Preparation of working electrodes

In this work, the properties of Ni₃CuN and Ni₃Cu were revealed by electrochemical measurements related to HER besides the above characterizations. The electrocatalyst ink was made from mixing 8 mg of powder, 50 μL of Nafion solution (5 wt. % in mixture of lower aliphatic alcohols and water, Merck) and 950 μL isopropanol (99.5%, Honeywell) into a glass vial and ultrasonicated for 30 min.

Aliquots of 10 μL of ink were drop-cast using a micropipette in a left-to-right sweeping motion, proceeding line by line from top to bottom to cover the working area ($1 \times 1 \text{ cm}^2$) of the raw carbon paper (Toray, TGP-H-60). This process was repeated until the working area was fully coated and the entire 100 μL of ink had been used. Finally, the drop-casted ink was allowed to dry in the ambient. The weight of the catalyst was obtained by approx. 0.9 mg.

Electrochemical measurement of hydrogen evolution reaction

The electrochemical measurements were carried out with an EC-Lab Biologic VSP potentiostat in an H-cell where the counter (anode chamber) and the working (cathode chamber) sides were separated by a FAA-3-PK-130 membrane (Fuel Cell Store) in alkaline conditions. All experiments were conducted in a 3-electrode configuration with a Pt foil ($1 \times 1 \text{ cm}^2$) as a counter electrode, Ag/AgCl (3.5 M KCl) as a reference electrode, and the carbon paper (Toray, TGP-H-60) coated with the catalyst as the working electrode. 25 mL of the electrolyte was filled into each chamber of the H-cell prior to the experiments. In this work, 1 M KOH (pH = 14) was applied as the electrolyte to compare the performance of two catalysts under alkaline conditions. In addition, linear sweep voltammetry (LSV) experiments were run within specific potential windows at 5 mV/s. All electrochemical experiments were corrected using an iR compensation of 85% *via* the automatic Biologic potentiostat function, and the cathode chamber was stirred at 300 rpm/min during all experiments. Typically, the potentials were converted to the reversible hydrogen electrode (RHE) with $E_{\text{RHE}} = E_{\text{Ag/AgCl}} + 0.205 \text{ V} + 0.059 \times \text{pH}$.

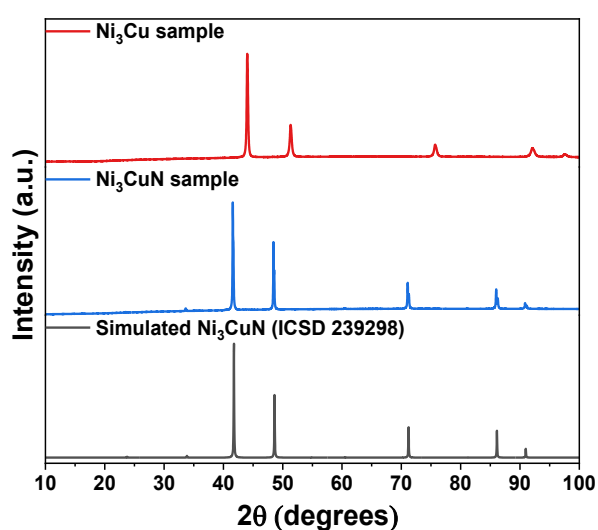


Fig. S1 The XRD pattern of Ni_3CuN (blue) of Ni_3Cu (red) in comparison with the simulated pattern for Ni_3CuN .¹

Table S1 The X-ray fluorescence measurement of Ni₃CuN and Ni₃Cu

Sample	Element	Theoretical molar percent (%)	The actual molar percent (%)
Ni ₃ CuN	Ni	75	74.30±0.02
	Cu	25	25.70±0.01
Ni ₃ Cu	Ni	75	74.40±0.02
	Cu	25	25.60±0.01

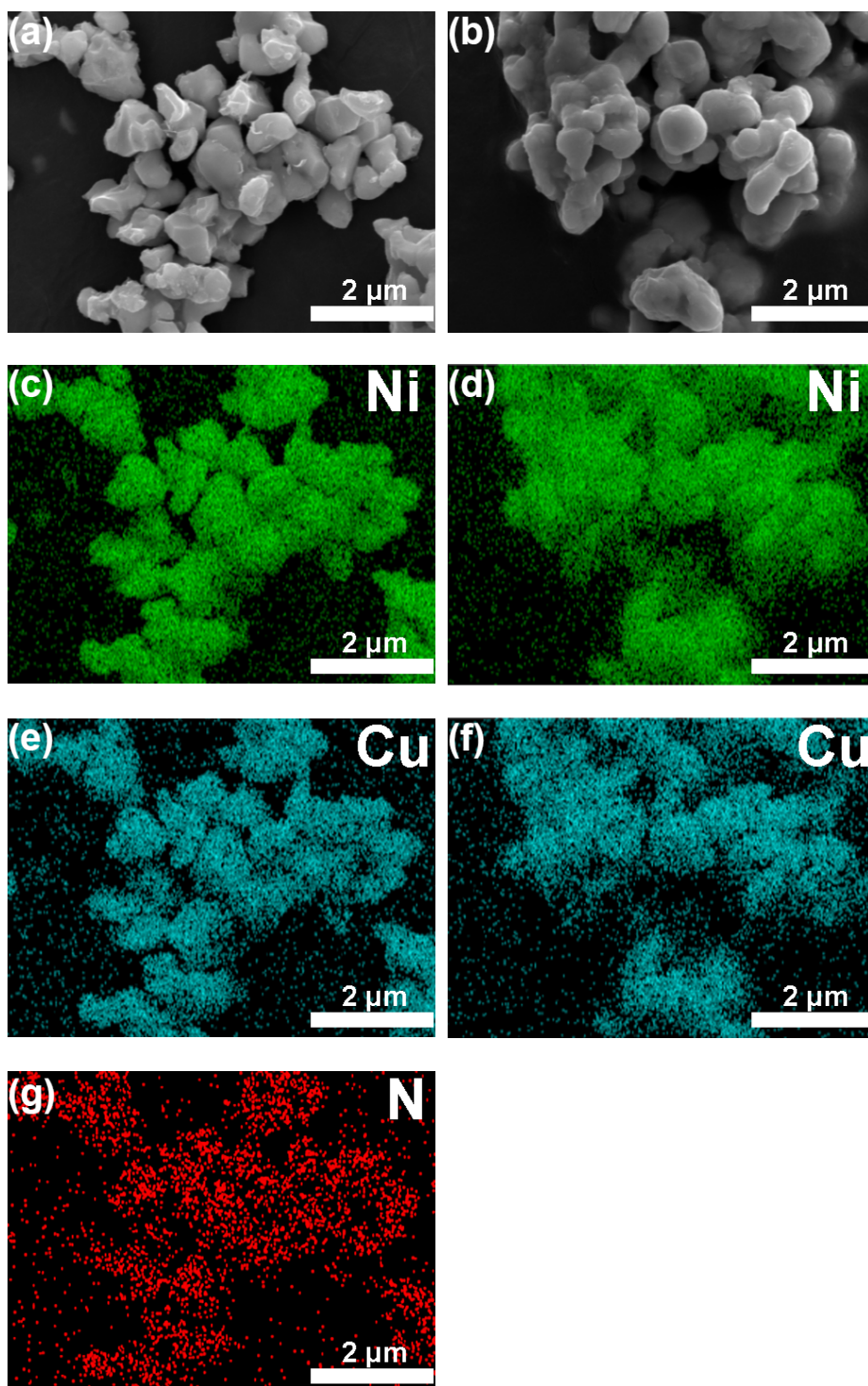


Fig. S2 SEM micrographs and corresponding EDS elemental maps of Ni_3CuN and Ni_3Cu . Panels (a) and (b) show the surface morphology of Ni_3CuN and Ni_3Cu , revealing submicron particle sizes with distinct textural differences. Panels (c) and (d) display the spatial distribution of Ni, while (e) and (f) show the distribution of Cu. The elemental maps confirm a homogeneous distribution of both elements across the respective samples. Panel (g) shows the uniform distribution of nitrogen in Ni_3CuN powder.

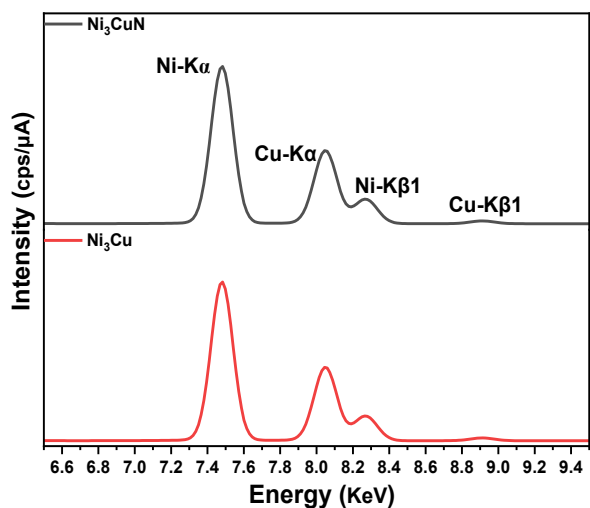


Fig. S3 The experimental XRF spectra of Ni₃CuN (grey) and Ni₃Cu (red) powders. The result showed that both nitride and alloy have the same relative peak intensities on Ni and Cu elements suggesting there was no ratio loss happened to Ni₃Cu.

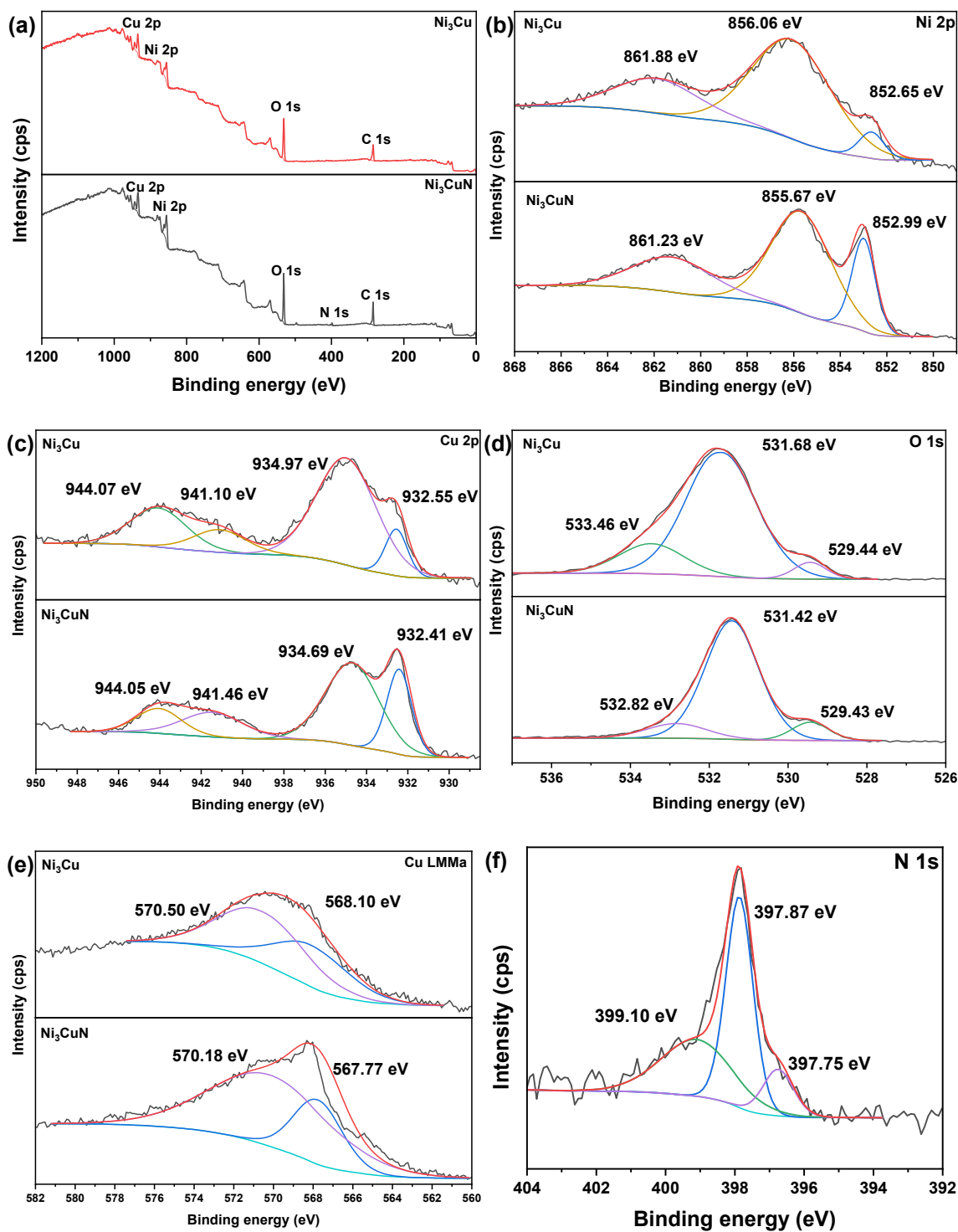


Fig. S4 The XPS spectra of Ni_3CuN and Ni_3Cu powders mounted on carbon adhesive tape including (a) Survey spectra and high-resolution spectra of (b) Ni 2p, (c) Cu 2p, (d) O 1s, (e) Cu LMMa and (f) N 1s.

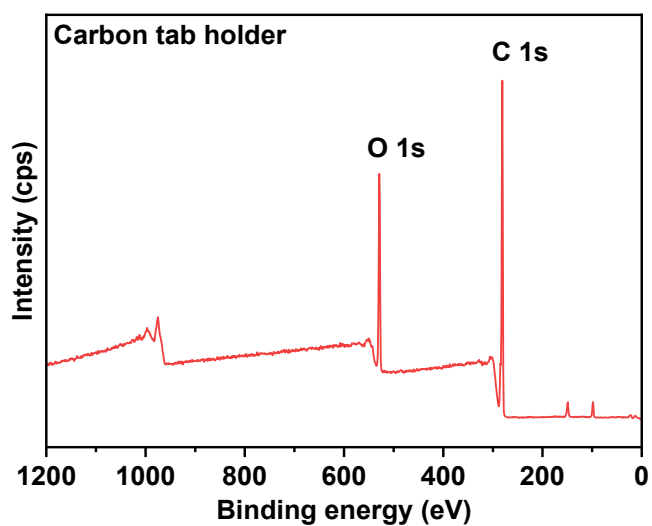


Fig. S5 XPS survey spectrum of the carbon tab holder.

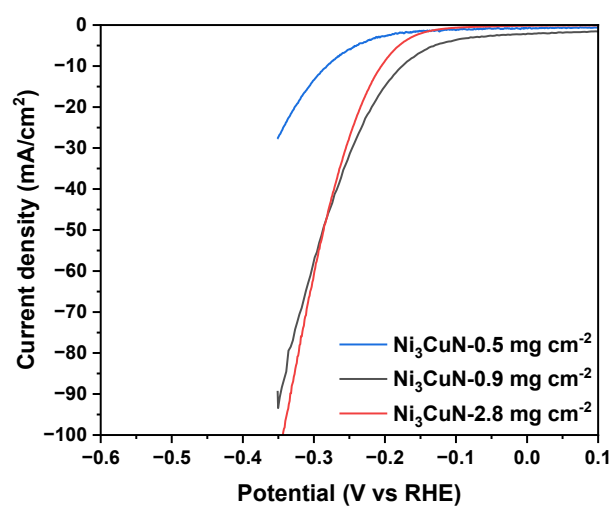


Fig. S6. The LSV curves of Ni_3CuN electrode with different mass loadings.

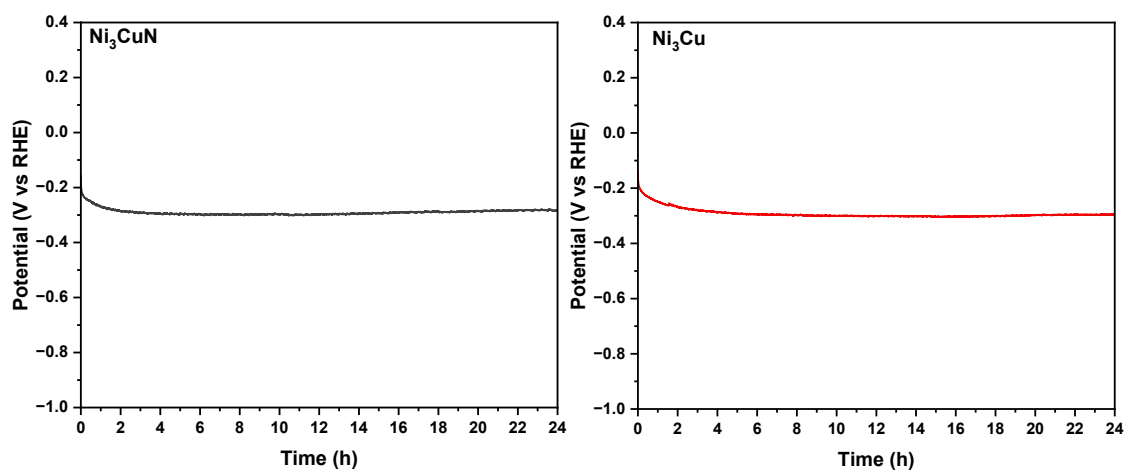


Fig. S7 The chronopotentiometry experiments at -10 mA/cm^2 of (a) Ni_3CuN and (b) Ni_3Cu in 1 M KOH for 24 hours

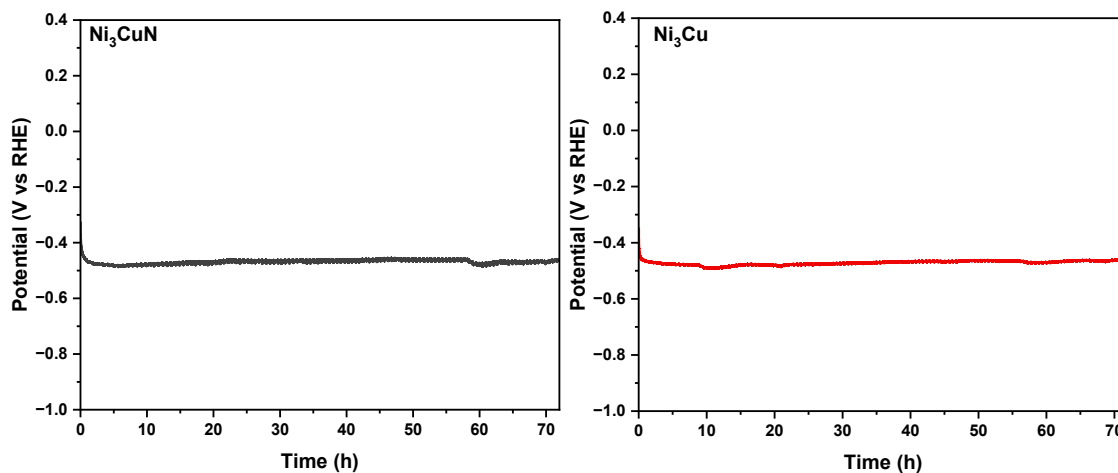


Fig. S8 The stability test of Ni_3CuN and Ni_3Cu for 72 hours in 1 M KOH at -50 mA/cm^2

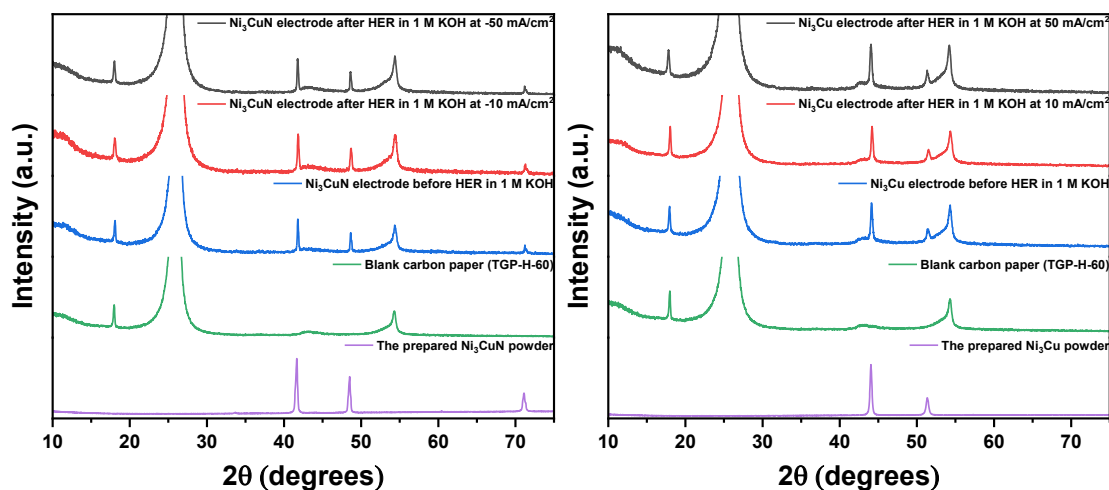


Fig. S9 The XRD patterns before and after HER experiments of (a) Ni_3CuN and (b) Ni_3Cu at -10 mA/cm^2 and -50 mA/cm^2 in 1 M KOH

Table S2 The ICP-OES measurements of the Ni_3CuN and Ni_3Cu after 24-hour HER in 1 M KOH

Experiments	Samples	Element	The leaching ratio
-10 mA/cm^2	Ni_3CuN	Ni	0
		Cu	$0.64 \pm 0.05 \text{ wt}\%$
	Ni_3Cu	Ni	0
		Cu	$0.11 \pm 0.06 \text{ wt}\%$
-50 mA/cm^2	Ni_3CuN	Ni	0
		Cu	$0.78 \pm 0.03 \text{ wt}\%$
	Ni_3Cu	Ni	0
		Cu	$0.51 \pm 0.01 \text{ wt}\%$

Reference

1. B. He, C. Dong, L. Yang, X. Chen, L. Ge, L. Mu and Y. Shi, *Superconductor Science and Technology*, 2013, **26**, 125015.